Article:
Romero, C.P., Ramirez-Mora, C., Salazar, R. orcid.org/0000-0002-2795-9348 et al. (5 more authors) (2026) Low-cost hybrid copper–carbon nanotube coating with antimicrobial properties in ambient conditions. Electronic Journal of Biotechnology, 79. 100700. ISSN: 0717-3458

https://doi.org/10.1016/j.ejbt.2025.100700

Electronic Journal of Biotechnology 79 (2026) 100700

Contents lists available at ScienceDirect

Electronic Journal of Biotechnology

journal homepage: www.elsevier.com/locate/ejbt

Short Communication

Low-cost hybrid copper–carbon nanotube coating with antimicrobial properties in ambient conditions ☆

Christian Pablo Romero [a,b,*], Claudio Ramirez-Mora [c], Rodolfo Salazar [d], Cristobal Fernandez [d], Cristian Acevedo [b], Christian Orellana [a], Maria Abellan [a], David Aliaga [e]

[a] Centro Científico Tecnológico de Valparaíso (CCTVAL), Av. General Bari 699, Valparaíso, Chile
[b] Departamento de Física, Universidad Técnica Federico Santa Maria, Av. España 1680, Valparaíso, Chile
[c] Naturatech SpA, Viña del Mar, Chile
[d] Departamento de Industrias, Universidad Técnica Federico Santa María, Av. España 1680, Valparaíso, Chile
[e] Department of Chemical and Biological Engineering, University of Sheffield, Mappin Street, Shimageeld, United Kingdom

GRAPHICAL ABSTRACT

Low-cost hybrid copper–carbon nanotube coating with antimicrobial properties in ambient conditions

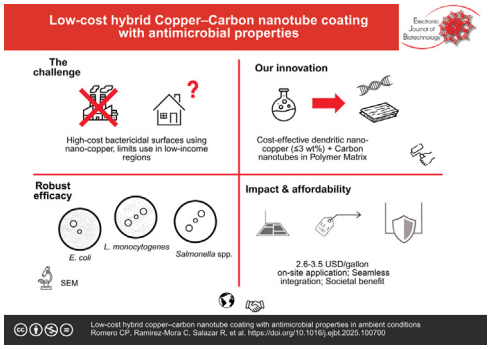

ARTICLE INFO

Article history:
Received 8 July 2025
Accepted 5 November 2025
Available online 4 December 2025

Keywords:
Carbon nanotubes
Cu
Low-cost coatings
Nanoparticles
Polymer matrix

ABSTRACT

Background: The development of bactericidal surfaces using nanotechnology has gained traction in high-tech sectors due to their effectiveness against pathogens. However, widespread adoption in low-income regions remains limited by the high cost of materials such as copper nanoparticles and the need for specialized application personnel. This study aims to develop a cost-effective bactericidal coating that minimizes nano-copper usage while maintaining strong antimicrobial performance and practical applicability in resource-limited environments.
Results: A polymer-based coating incorporating ≤3 wt% nano-copper and carbon nanotubes was formulated to enhance conductivity and mechanical stability. The fabrication process was optimized for on-site application under ambient conditions. Scanning Electron Microscopy (SEM) revealed a uniform surface distribution of nano-copper particles. Bactericidal activity tests confirmed efficacy against *Escherichia coli*, *Listeria monocytogenes*, and *Salmonella* spp. Techno-economic analysis indicated that the coating could be integrated into existing surface finishing systems at an incremental cost of 2.6–3.5 USD per gallon.
Conclusions: This work demonstrates the feasibility of producing and applying affordable nano-based

☆ Audio abstract available in Supplementary material.
Peer review under responsibility of Pontificia Universidad Católica de Valparaíso.

* Corresponding author.
E-mail address: christian.romero@usm.cl (C.P. Romero).

https://doi.org/10.1016/j.ejbt.2025.100700

bactericidal coatings under real-world conditions. The approach provides a practical pathway for implementing antimicrobial surface technologies in low-resource settings. Although the present study focused on wood substrates, future research should assess performance on diverse materials to broaden applicability. The combination of cost-effectiveness, efficacy, and scalability underscores the potential for both commercial adoption and significant public health benefits.

How to cite: Romero CP, Ramirez-Mora C, Salazar R, et al. Low-cost hybrid copper–carbon nanotube coating with antimicrobial properties in ambient conditions. Electron J Biotechnol 2026;79. https://doi.org/10.1016/j.ejbt.2025.100700.

1. Introduction

It is well established that bactericidal surface treatments have increasingly adopted hybrid material approaches. Over the past five decades, materials science has undergone sustained development and diverse research efforts, particularly in the development and application of nanomaterials. Nanoparticles, for instance, have been utilized in a wide range of fields, including the fabrication of nanocomposite scaffolds for biomedical applications [1]. Surface potential is not only relevant to bactericidal properties research. In general, the surface kinetics are dominated by how species are absorbed at the interphase and how these surface potentials interact with an incoming atoms or molecules. Much research has been done, ranging from bactericidal studies to for example hydrogen adsorption on metallic systems [2], among many other areas and topics.

Bactericidal surface treatments are critical for preventing bacterial infections in medical, industrial, and domestic settings. These treatments are designed to inhibit bacterial adhesion, growth, and proliferation by integrating antimicrobial agents into surfaces or modifying surface properties to enhance their bactericidal efficacy [3]. The demand for such treatments has risen with increasing concerns over hospital-acquired infections (HAIs) and the emergence of antibiotic-resistant bacteria [4]. Similarly, virucidal surface treatments have become an essential focus in infection control, particularly in response to viral outbreaks such as COVID-19. These treatments aim to inactivate or destroy viruses upon contact, reducing transmission risks in healthcare, public, and domestic environments [5]. Virucidal coatings and materials play a crucial role in enhancing hygiene protocols by providing continuous antiviral activity and minimizing surface-mediated viral spread [6].

Low-cost bactericidal and virucidal surface treatments are especially valuable in resource-limited settings. Affordable antimicrobial solutions, such as copper-infused coatings, silver nanoparticles, and plant-based extracts, have shown significant promise due to their broad-spectrum efficacy and accessibility [7,8]. Copper-based paints and varnishes, which require minimal amounts of metal while maintaining antimicrobial properties, present a cost-effective and scalable alternative to conventional disinfection methods [9]. The integration of carbon nanotubes with copper composites has demonstrated enhanced bactericidal activity with low material costs [10]. Natural compounds, such as essential oils and flavonoids, offer another sustainable and inexpensive solution, particularly in rural areas where synthetic antimicrobial agents may be inaccessible [11]. These innovations provide affordable, durable, and effective means of reducing microbial contamination and mitigating disease transmission in the developing world.

Bactericidal surface treatments function via diverse mechanisms. Chemical release mechanisms are widely used, some surfaces incorporate antimicrobial agents such as silver nanoparticles, copper coatings, or quaternary ammonium compounds, which gradually release ions that disrupt bacterial cell membranes and metabolic processes [12]. The contact-killing mechanisms is an electrical effect, certain surfaces, such as those modified with cationic polymers, kill bacteria upon direct contact by disrupting the integrity of bacterial membranes through electrostatic interactions [13]. The surface potential can also be modified via surface nano-structuring, in this case emerging technologies include nano-patterned surfaces inspired by natural antimicrobial surfaces, such as insect wings. These surfaces physically rupture bacterial membranes through mechanical stress, preventing bacterial colonization [14]. Then there are the photon absorbing materials like the photo-activated antimicrobial surfaces. These surfaces coated with photosensitive materials like titanium dioxide generate reactive oxygen species (ROS) under light exposure, leading to oxidative damage to bacterial cells [15].

Recent advances in bactericidal and virucidal surface treatments focus on improving efficiency, durability, and environmental sustainability. In the case of graphene-based coatings, both graphene oxide and reduced graphene oxide coatings exhibit strong antimicrobial properties due to their ability to induce oxidative stress and physical damage in bacterial membranes [16]. The bio-inspired antimicrobial surfaces, where scientists mimic antimicrobial structures found in nature, such as cicada and dragonfly wings, to create self-cleaning and highly effective bactericidal materials [17]. Further approaches worth mentioning are the stimuli-responsive antimicrobial surfaces, here the concept of smart surfaces that can respond to environmental cues, such as pH or temperature changes, have been designed to release antimicrobial agents on demand, reducing the risk of bacterial resistance development [18]. In this same category are the hybrid antiviral technologies: Combining multiple antiviral mechanisms, such as metal ions with photocatalytic activity, enhances the efficiency and longevity of virucidal coatings [19].

Although many materials are available, one that stands out is copper, it is relatively abundant, but the cost has increased over time. Here nano sized copper has emerged as a highly effective material for bactericidal surface treatments due to its intrinsic antimicrobial properties. Copper and its alloys, such as brass and bronze, have been widely utilized in healthcare, food processing, and public spaces to reduce bacterial contamination and prevent infections. The ability of copper to kill bacteria is attributed to multiple mechanisms, including direct membrane damage, generation of ROS, and interference with essential cellular processes [9]. Copper surfaces exhibit rapid and broad-spectrum antimicrobial activity against both Gram-positive and Gram-negative bacteria, including antibiotic-resistant strains such as methicillin-resistant *Staphylococcus aureus* (MRSA) and *Escherichia coli* [10]. The continuous antimicrobial action of copper reduces biofilm formation and enhances hygiene in frequently touched surfaces, such as door

handles, railings, and medical instruments [11]. Recent advances in copper-based surface modifications, including nano-coatings and composites, further enhance the durability and effectiveness of bactericidal properties [9]. The integration of copper into high-touch surfaces offers a sustainable and cost-effective strategy for infection control and improved public health.

A key limitation of existing state-of-the-art solutions (as described above) is that they rarely reach low-income communities and countries. In contrast, this work aims to deliver a practical, low-cost alternative with straightforward steps – accessible to households at all income levels. To ensure real-world applicability, the method was implemented entirely by hand under everyday conditions, minimizing reliance on specialized equipment or laboratory settings.

In this work, we test a low-cost procedure to demonstrate that a novel copper-based composite, incorporating carbon nanotubes, exhibits enhanced bactericidal and virucidal properties compared to untreated surfaces. The primary advancement of this research lies in the utilization of a minimal concentration of copper particles, synergistically combined with charge-transferring carbon nanotubes, to develop a transparent, slightly conductive coating. This coating, formulated as a paint-like substance, can be applied as a conventional varnish on a wide range of surfaces, this offers a cost-effective and scalable solution for antimicrobial protection. Included in this work we provide a list with specific steps to obtain an active antimicrobial surface.

2. Methods

Samples were prepared using a basic proprietary formulation containing Cu nanoparticles, single-walled carbon nanotubes (SWCNTs) bought from the company Tuball (https://www.tuball.com) and a resin. The formulation was designed to meet the following criteria: (a) minimal utilization of Cu nanoparticles to reduce cost, as Cu nano particles represent the highest cost in any coating carrying these nano particles, in this work ≤3 wt% was used, (b) production of a coating that does not exhibit a metallic appearance or a copper-like coloration, and (c) maintenance of low electrical conductivity.

Multiple sets of samples were fabricated under consistent conditions. The application process involved the use of a one-inch paintbrush to uniformly coat the substrate surfaces with the formulated substance. Following application, the samples were allowed to dry for 24 h under ambient conditions (22°C and 30% relative humidity). The substrate material (wood) was cleaned only to remove dust prior to coating, without additional surface treatment, to ensure the sample preparation closely resembled real-world application conditions.

A total of 36 sample spaces were produced, all with the same surface treatment. The application of the active layer on the surfaces can be seen in Fig. 1.

The main steps to develop this coating are listed here in this paragraph, these steps may be modified for other specific applications.

1) Coating base: The coating is based on a two-component monomer, specifically designed to prevent premature polymerization during the dispersion of single-walled carbon nanotubes, which act as a structural modification agent of the polymer. The first component of the monomer acts as a vehicle to disperse the nanotubes without initiating the polymerization reaction. Only after this dispersion is complete can the catalyst be added.
2) Carbon nanotube dispersion: Use a Cowles-type agitation system in a cylindrical vessel with a flat bottom. Disperse carbon nanotubes in an initial stage at a 1:49 ratio relative to the base monomer (e.g., 4 g in 196 g of resin). Mix at a peripheral speed between 7 and 10 m/s for 20 min. Then add the rest of the monomer (final dilution) and mix for an additional 5 min at the same speed.
3) Catalyst addition: Add peroxide to the monomer once the carbon dispersion is complete. This peroxide acts as the polymerization catalyst.
4) Incorporation of dendritic copper: Before polymerization progresses too far, making further additions difficult, add 3% dendritic copper particles. These particles must be dendritic (never spherical), as their geometry prevents sedimentation and ensures a homogeneous distribution throughout the polymer layer.
5) Active component: Add dendritic copper powder with a particle size of approximately 6 μm. Its low apparent density facilitates uniform suspension in the polymer.
6) Material ratio (per 200 g batch of monomer): 200 g of monomer, 10 g of peroxide (5%). Ensure that adequate mass of dendritic copper for the desired outcome of the application.
7) Coloring and visual identification (optional): To aid in identifying the painted area, a mix of copper and tin powder can be added. This gives the coating a distinctive color without affecting its functional properties.
8) Application and masking tape removal: Apply the mixture uniformly on the wood substrate. Remove masking tape strips approximately 5 min after application, before the coating begins to dry, to prevent tearing or adhesion.

The techno-economic analysis indicates that this coating can be incorporated into existing floor and wall finishes, with an estimated incremental cost ranging from 2.6 to 3.5 USD per gallon.

3. Characterization

To characterize the samples and their layout, scanning electron microscopy (SEM) was used. These results are shown in Fig. 2 and Fig. 3.

Analysis of Fig. 2 reveals that the dendritic copper distribution has a maximum copper-free diameter of 450 nm (indicated by red annotation). Quantitative characterization was performed using ImageJ software (v1.53 m, NIH) following standard image processing protocols. The surface coverage analysis yielded an estimated free surface area of 83 ± 5%, determined through threshold-based particle analysis (Fig. 3, inset). This measurement accounts for the inherent sensitivity of threshold selection, where incremental parameter adjustments (± 2.5% threshold level variation) produced a 5% fluctuation in calculated free surface area, a systematic error incorporated into our reported values. The edge detection algorithm, shown in Fig. 2, demonstrated robust performance, with clearly defined boundaries between copper deposits and the substrate matrix. This facilitated accurate binary segmentation and subsequent morphometric analysis. The observed threshold sensitivity underscores the importance of standardized image processing parameters for reproducible quantification of surface coverage characteristics.

The samples were analyzed using a Thermo Scientific ESEM Quattro S scanning electron microscope at the University of Valparaíso's "Hub Microscopía" facility (Chile). Standard SEM imaging conditions were employed, with conventional vacuum operation selected a priori, due to the conductive nature of the samples.

Image analysis revealed a non-uniform distribution of dendritic Cu nanoparticles across the surface, with localized agglomerations. Nevertheless, there was no larger surface area without some degree of dendritic copper particles as shown in Fig. 2. While the obtained resolution adequately captured the particles' structural

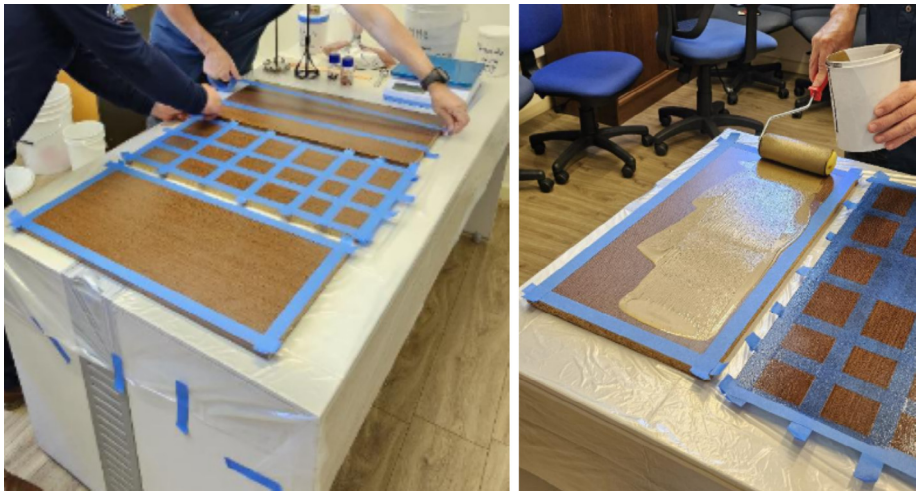

Fig. 1. The images show the sample preparation on the wood substrate in regular indoor ambient conditions.

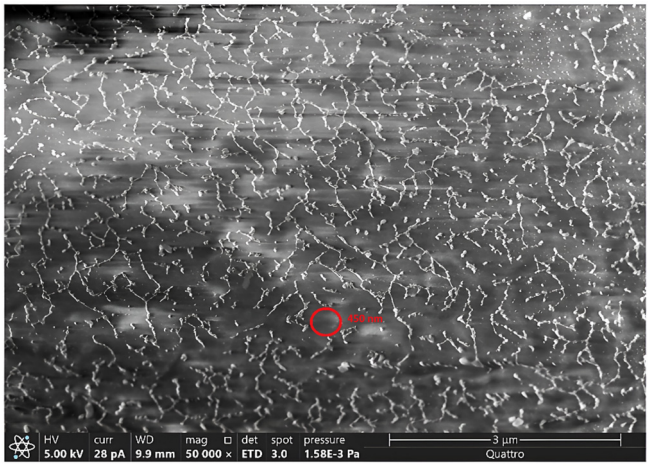

Fig. 2. Representative SEM image, where the Cu nano particles are visible in a dendritic layout on the surface. Scale set to 3 µm. Largest diameter with no visible dendritic copper ranges at 450 nm, shown in red. (For interpretation of the references to colour in this figure legend, the reader is referred to the web version of this article).

characteristics, significant charge accumulation occurred during imaging, more than expected, thus proving that the conductive nature of the samples where not sufficient to dissipate all the charge buildup from the electron beam.

Characterization of the dendritic copper was also performed. Fig. 4 and Fig. 5 show an SEM image of the dendritic copper. Table 1 and Table 2, show the Energy Dispersive Spectroscopy (EDS) results of the analysis of the dendritic copper composition.

The data in Table 1 and Table 2, demonstrate that the dendritic copper flakes are metallic.

The full characterization of the system (dendritic copper + SWCNT + resin) was conducted using Raman Spectroscopy. We employed a Modular Micro Raman Confocal RENISHAW-SPECTROMETER system, with a visible light excitation source of 532 nm (Fig. 6).

The most characteristic Raman-active mode of cuprite is observed at approximately 218 cm^{-1}, corresponding to the second order Raman mode, strong and sharp. This is considered the fundamental fingerprint of Cu_2O in Raman spectroscopy and corresponds to the vibration of the Cu—O bond. In addition to the primary peak, several higher-order and overtone bands are typically observed: 145, 412, 630 cm^{-1}.

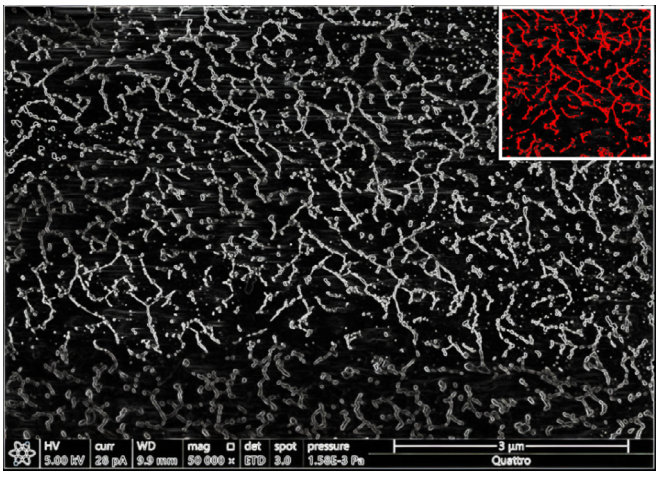

Fig. 3. Shows post produced image for clear edge identification using ImageJ software. The inset shows the effect of Color Threshold post processing to calculate the average surface without dendritic copper.

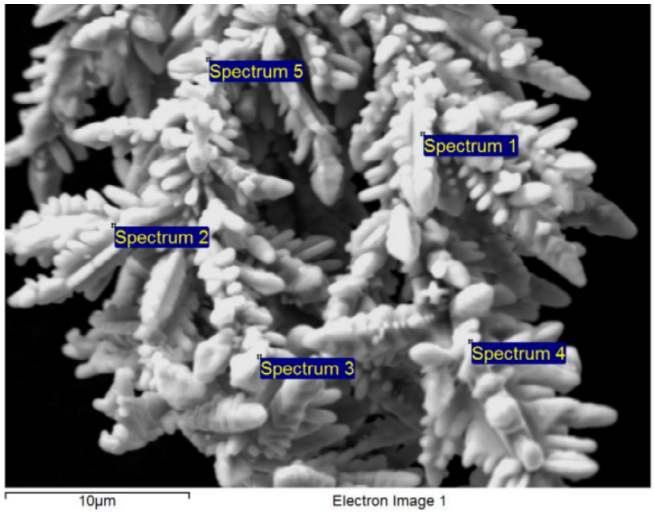

Fig. 4. Closeup SEM image of one dendritic copper flake used to elaborate the coating.

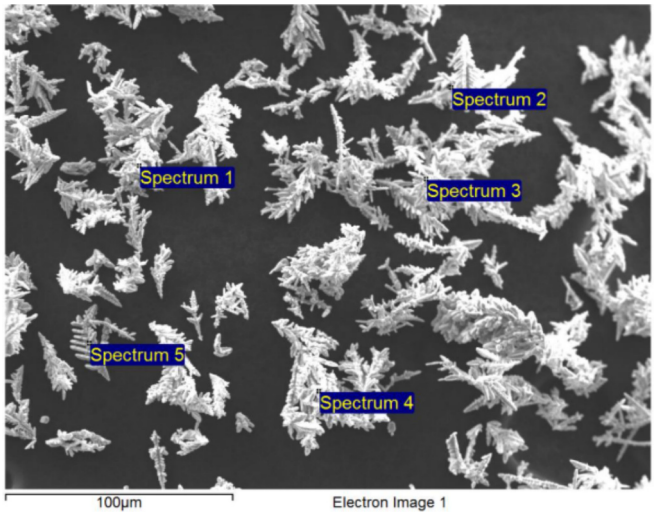

Fig. 5. SEM of several dendritic copper flakes and the location of EDS.

The relative intensity and peaks position may vary slightly depending on crystallinity, particle size, strain, and the excitation wavelength used during Raman measurement. However, the presence of the ~218 cm^{-1} mode remains the most reliable marker for identifying cuprite, thus the presence of Cu^{+2}. The Raman analysis supports that the low oxygen levels detected in the EDS indicate a thin layer of cuprite (Cu_2O) on the surface.

4. Experimental procedure

Two sets of surface samples were prepared within a single large test area, as illustrated in Fig. 1. Additionally, two more surfaces were prepared and divided into rectangular zones, also shown in Fig. 1. The large, undivided area was designated as the control sample throughout all experiments.

Three microbial strains were selected for testing, based on their high prevalence in common environments and relevance to food safety. All procedures were conducted in accordance with the Chilean sanitary regulation IM78 Rev.3, issued by the Ministry of Health. The selected aerobic mesophilic microorganisms were *E. coli*, *Listeria monocytogenes*, and *Salmonella* spp.

The IM78 Rev.3 standard defines permissible microbiological limits for surfaces that come into contact with food, aiming to ensure food hygiene and safety across production, processing, and handling operations. Enforced by Chile's Health Authority, the regulation emphasizes the evaluation of surface cleanliness via microbial load quantification. According to this standard, one key microbiological indicator is Aerobic Mesophilic Count (AMC) must be <100 CFU/cm^2. The standard further specifies validated sampling methodologies, analytical procedures, and adherence to good laboratory practices.

Sample preparation was carried out by the research team under ambient laboratory conditions. All microbiological analyses were performed by the certified laboratory SiLob Chile, located in Valparaíso, Chile. Additional information on their services is available at: https://www.silobchile.cl. Each test was performed in triplicate to ensure reproducibility and statistical reliability. Reported values for each microorganism represent the average of three independent measurements. Initial bacterial deposition was conducted on all surfaces, followed by microbial re-counts at defined time intervals, as detailed in Table 3.

At each time interval specified in Table 3, a quantitative bacterial count was performed. This measurement follows standard microbiological procedures commonly applied to food, water, and surfaces in contact with food, as outlined in Chilean regulation IM78 Rev.3. The assessment was conducted using culture-based methods that quantify microbial load in terms of colony forming units (CFU) per square centimeter (CFU/cm^2) or per gram (CFU/g), depending on the sample type.

The initial inoculum concentrations applied to the surface were 2.1×10^2 CFU/mL of *E. coli* (±0.3), 1.2×10^3 CFU/mL of Listeria (±0.2), and 1.2×10^2 CFU/mL of *Salmonella* (±0.5). After inoculation, the bacterial suspensions were allowed to dry on the surface. Samples were then collected using swabs and diluted in water. The specific time intervals for sample collection are presented in Table 3. Neutralization was not conducted, as the surface does not release or desorb any known chemical compounds.

5. Results and discussion

Fig. 7, Fig. 8 and Fig. 9 present the temporal evolution of bacterial colony counts for the three selected species. CFU counts are plotted over time to evaluate microbial survival on the various test surfaces. Fig. 7 illustrates the behavior of *E. coli* on the different surface samples. A significant reduction in CFU count is observed for the treated surfaces (represented by the red and grey lines), relative to the control surface (black line). Notably, the treated surfaces exhibited a rapid decline in bacterial load, falling below the regulatory threshold of 100 CFU/cm^2 within the first 30 min. In contrast, the control surface only reached this threshold after approximately 1 h. Additionally, all surface types showed further bacterial reduction over time, with CFU counts dropping below 15 CFU/cm^2 by the 6 h mark. Subset A exhibited the most rapid antimicrobial activity, reaching this low bacterial count within just 30 min.

Fig. 8 depicts the temporal reduction of *L. monocytogenes* CFU across the different test surfaces. A progressive decline in microbial load is observed for all samples over time. Notably, both treated surfaces (Subset A and Subset B) exhibited a more pronounced and rapid reduction compared to the control.

Subset A (red line) showed a decrease from 1390 CFU/cm^2 to 337 CFU/cm^2 within the first hour, while Subset B (gray line) declined from 1240 CFU/cm^2 to 180 CFU/cm^2 in the same timeframe. In contrast, the control surface exhibited a more gradual

Table 1
Shows the atomic composition in weight % of the EDS spectrum on all 5 locations of the dendritic copper.

Elemental analysis (Normalized)				
Spectrum	**In stats.**	**O**	**Cu**	**Total**
Spectrum 1	Yes	1.86	98.14	100
Spectrum 2	Yes	1.24	98.76	100
Spectrum 3	Yes	3.27	96.73	100
Spectrum 4	Yes	3.16	96.84	100
Spectrum 5	Yes	1.69	98.31	100
Mean		**2.24**	**97.76**	**100**

Table 2
Show the atomic composition in weight % of the EDS spectrum on all 5 locations of the different dendritic copper flakes.

Elemental analysis (Normalized)				
Spectrum	**In stats.**	**O**	**Cu**	**Total**
Spectrum 1	Yes	1.44	98.56	100
Spectrum 2	Yes	1.98	98.02	100
Spectrum 3	Yes	0.63	99.37	100
Spectrum 4	Yes	0.53	99.47	100
Spectrum 5	Yes	0.23	99.77	100
Mean		**0.96**	**99.04**	**100**

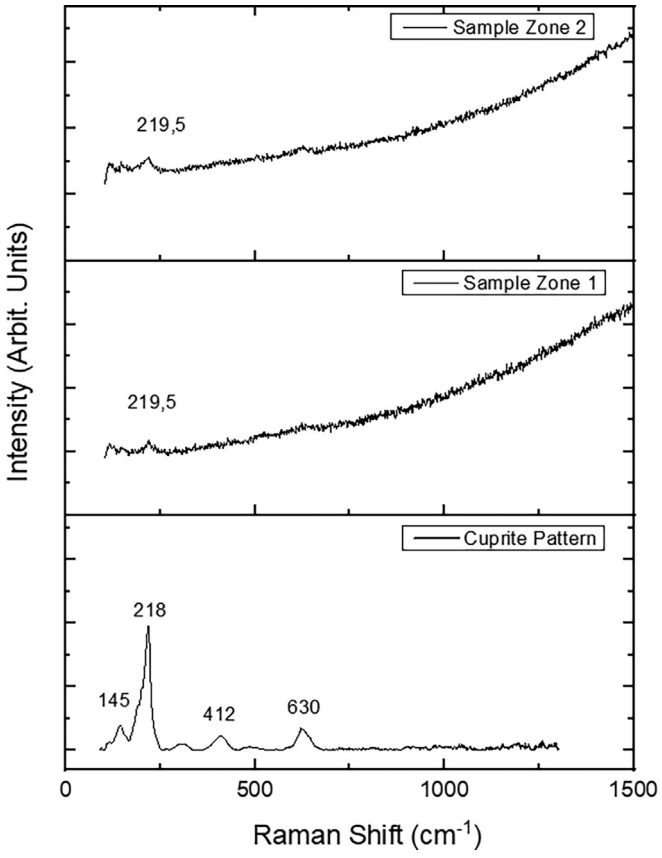

Fig. 6. RAMAN spectra of samples measured at room temperature in the range 0–1500 cm^{-1}, compared with cuprite pattern.

Table 3
Time when bacteria recount was performed during the experiment.

Time	Unit
0	min
30	min
60	min
360	min
1440	min

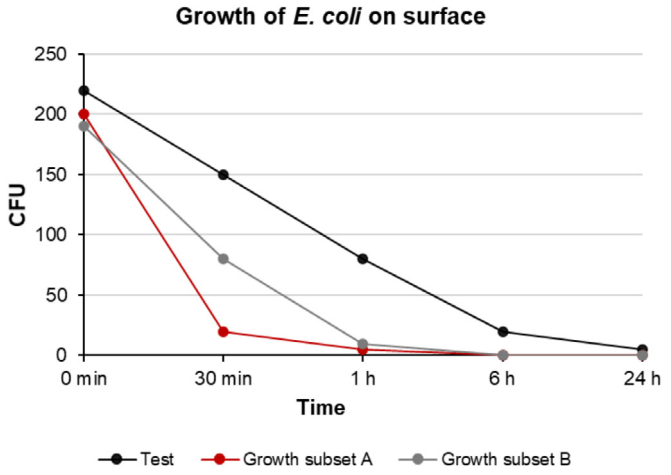

Fig. 7. Shows *E. coli* colony forming units versus time. The black line depicts the test sample without surface treatment.

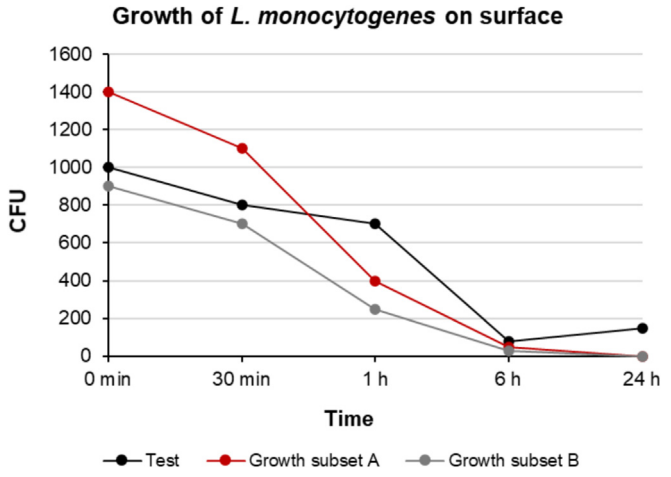

Fig. 8. Shows *L. monocytogenes* colony forming units versus time. The black line depicts the test sample without surface treatment.

decline, with CFU counts dropping from 1076 to 716 CFU/cm^2 during the first hour.

The bacterial load on Subsets A and B fell below the 100 CFU/cm^2 threshold after approximately 5 h, whereas the control sample reached this level only after 6 h. At the 24-h mark, Subsets A and B maintained minimal bacterial presence, with CFU counts remaining below 25, whereas the control surface still exhibited a count of approximately 150 CFU/cm^2. These results highlight the enhanced antimicrobial efficacy of the treated surfaces compared to the untreated control.

Fig. 9 illustrates the temporal reduction in *Salmonella* spp. colony-forming units (CFU) across the various surface samples. A gradual decline in bacterial counts is observed for all surfaces over the duration of the experiment. Treated surfaces (Subsets A and B) demonstrated moderate antimicrobial activity, with CFU counts decreasing to below 100 CFU/cm^2 at approximately 6 h. In contrast, the untreated control surface did not reach this threshold at any time point during the 24 h observation period.

By the 24 h mark, all three surfaces –treated and untreated- exhibited CFU levels at or above 100 CFU/cm^2, indicating a resur-

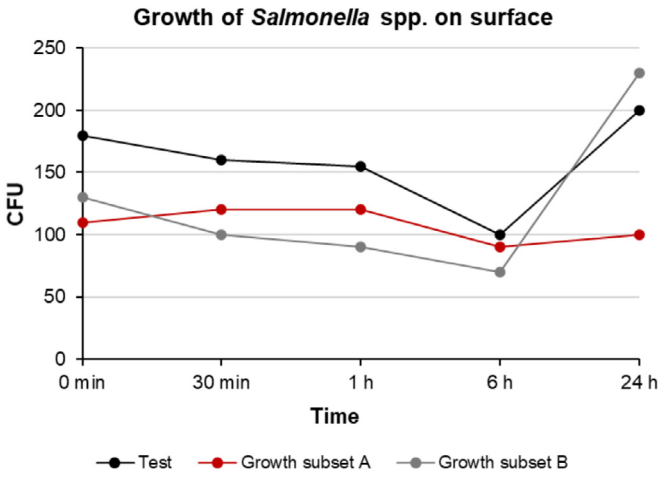

Fig. 9. Shows *Salmonella* colony forming units versus time. The black line depicts the test sample without surface treatment.

gence or persistence of viable *Salmonella* cells over extended periods. These results suggest that while the treated surfaces provide temporary suppression of *Salmonella* proliferation, their long-term antimicrobial efficacy against this particular microorganism is limited compared to their performance against *E. coli* and *L. monocytogenes*.

Although both *E. coli* and *Salmonella* are Gram-negative bacteria, the surface appears to inhibit the proliferation of *E. coli* but not *Salmonella*. This differential response may be attributed to structural differences in their outer membranes, particularly the O-antigen component of lipopolysaccharides. *Salmonella* is known to possess longer and more complex O-antigen chains, which can contribute to a higher negative surface charge compared to *E. coli*, potentially affecting interactions with the surface material [20]. However, this study did not include membrane permeability assays (e.g., LIVE/DEAD staining) or surface charge characterization through zeta potential measurements, which could provide valuable insights into the mechanisms underlying the observed bactericidal activity.

The synergistic combination of electronically donating dendritic copper particles embedded in a semiconductive polymer-carbon nanotube matrix creates a multifunctional composite system with antimicrobial properties. Experimental characterization reveals substantial bactericidal activity despite the remarkably low copper nanoparticle concentration (≤3 wt%) incorporated in the coating formulation. This enhanced performance appears to originate from three interconnected mechanisms: first, the carbon nanotube network facilitates efficient charge transfer throughout the matrix; second, the dendritic copper morphology provides increased effective surface area; and third, optimized electrochemical activity occurs at the copper-polymer interface. The demonstrated antimicrobial efficacy suggests the system operates primarily through an electron-mediated mechanism rather than relying solely on conventional copper ion release. These findings indicate promising potential for developing effective, low-copper-content antimicrobial coatings where the conductive substrate actively contributes to the biocidal functionality through charge transfer phenomena.

Long term stability of this coating has not been performed in this work, for further commercial application long term stability studies must be carried out. Although the coating exhibits a pronounced bactericidal effect, it remains unclear to what extent this activity arises from the synergistic interaction between SWCNTs and dendritic copper particles, or whether it is predominantly attributable to SWCNTs alone. Further investigations are required to elucidate this important aspect.

6. Conclusions

This low-cost antimicrobial coating developed in this study was evaluated for its effectiveness in inhibiting aerobic mesophilic bacterial growth on treated surfaces. The microorganisms selected for testing *E. coli*, *L. monocytogenes*, and *Salmonella* spp. were chosen due to their relevance in food safety and prevalence in food processing environments.

The coating was applied under standard ambient conditions without specialized surface pre-treatment, apart from basic dust removal from industrial wood substrates. Surface characterization using SEM confirmed the presence of dendritic copper particles uniformly distributed across the surface. The embedded SWCNTs were not visible under SEM, as they were homogenized within the polymer matrix. The SEM images show the presence of dendritic copper was distributed over all the surfaces. The largest area with no or little copper was a circular area with a diameter of 450 nm approximately. The copper free area as visible from the SEM images was estimated to be 83%. To enhance uniformity in future coatings, it is recommended to optimize the homogenization protocol during the dispersion phase. Improved mixing techniques could contribute to more consistent particle distribution and reduce agglomeration, thereby improving both the physical and functional properties of the coating.

The surface application protocol was done deliberately to mimic the real-life conditions in normal household conditions. No laboratory preparations were done on the surface apart from removing dust accumulation with a cloth. The results demonstrated notable antimicrobial efficacy against *E. coli* and also *L. monocytogenes*. In particular, E. coli colony counts on treated surfaces fell below the Chilean regulatory limit of 100 CFU/cm^2 in under 27 min, compared to 1 h on the untreated control, representing a 55 % reduction in time to compliance. Similar trends were observed for *L. monocytogenes*, where both treated surfaces exhibited faster and more sustained reductions in bacterial counts compared to the control.

In contrast, the results for *Salmonella* spp. were less conclusive. While treated surfaces showed a reduction in CFU counts during the first 6 h, bacterial levels increased thereafter across all surfaces, including the control. These findings suggest that although the coating exhibits initial inhibitory effects, its long-term effectiveness against *Salmonella* may be limited. Further research, including extended-duration studies and formulation optimization, is recommended to improve efficacy against this microorganism.

The data of this report suggest that it is possible to manufacture low-cost coatings in rustic settings, that decreases the bacterial growth when applied to wood surfaces, reaching bacterial counts bellow the Chilean regulatory limit.

CRediT authorship contribution statement

Christian Pablo Romero: Writing – review & editing, Writing – original draft, Supervision, Software, Resources, Project administration, Methodology, Investigation, Formal analysis, Data curation, Conceptualization. **Claudio Ramirez-Mora:** Writing – review & editing, Investigation, Funding acquisition, Data curation, Conceptualization. **Rodolfo Salazar:** Resources, Formal analysis. **Cristobal Fernandez:** Writing – review & editing, Investigation, Formal analysis, Data curation, Conceptualization. **Cristian Acevedo:** Investigation, Formal analysis. **Christian Orellana:** Software, Data curation. **Maria Abellan:** Visualization, Validation. **David Aliaga:** Writing – review & editing, Formal analysis, Data curation, Conceptualization.

Declaration of Generative AI and AI-assisted technologies in the writing process

During the preparation of this work the author(s) used Deepseek in order to harmonize the English text. After using this tool,

the author(s) reviewed and edited the content as needed and take (s) full responsibility for the content of the publication.

Financial support

C.P. Romero, C. Orellana and M. Abellan acknowledge the financial support received by ANID PIA/APOYO AFB230003.

Data availability

No data was used for the research described in the article.

Declaration of competing interest

We, the authors of this manuscript have no conflict of interest.

Acknowledgments

The authors acknowledge the support of CCTVAL and Universidad Técnica Federico Santa Maria, Valparaiso, Chile.

Supplementary material

Supplementary data to this article can be found online at https://doi.org/10.1016/j.ejbt.2025.100700.

References

[1] Catalan KN, Corrales TP, Forero JC, et al. Glass transition in crosslinked nanocomposite scaffolds of gelatin/chitosan/hydroxyapatite. Polymers 2019;11(4):642. https://doi.org/10.3390/polym11040642. PMid: 30970604.
[2] Romero CP, Avila JI, Trabol RA, et al. Pd as a promoter to reduce Co cluster films at room temperature. Int J Hydrogen Energy 2010;35(6):2262–7. https://doi.org/10.1016/j.ijhydene.2010.01.026.
[3] Hasan J, Crawford RJ, Ivanova EP. Antibacterial surfaces: The quest for a new generation of biomaterials. Trends Biotechnol 2019;37(5):295–304. https://doi.org/10.1016/j.tibtech.2013.01.017.
[4] Su Q, Xue Y, Wang C, et al. Strategies and applications of antibacterial surface-modified biomaterials. Bioact Mater 2025;53:114–40. https://doi.org/10.1016/j.bioactmat.2025.07.009. PMid: 40688018.
[5] Górny R, Gołofit-Szymczak M, Pawlak A, et al. Effectiveness of UV-C radiation in inactivation of microorganisms on materials with different surface structures. Ann Agric Environ Med 2024;31(2):287–93. https://doi.org/10.26444/aaem/189695. PMid: 38940114.
[6] Jefferson T, Del Mar C, Dooley L, et al. Physical interventions to interrupt or reduce the spread of respiratory viruses. Cochrane Database Syst Rev 2020;20(11):CD006207. https://doi.org/10.1002/14651858.CD006207.pub5. PMid: 33215698.
[7] Vincent M, Hartemann P, Engels-Deutsch M. Antimicrobial applications of copper. Int J Hyg Environ Health 2016;219(7):585–91. https://doi.org/10.1016/j.ijheh.2016.06.003. PMid: 27318723.
[8] Montero DA, Arellano C, Pardo M, et al. Antimicrobial properties of a novel copper-based composite coating with potential for use in healthcare facilities. Antimicrob Resist Infect Control 2019;8:3. https://doi.org/10.1186/s13756-018-0456-4. PMid: 30627427.
[9] Warnes SL, Caves V, Keevil CW. Mechanism of copper surface toxicity in *Escherichia coli* O157:H7 and *Salmonella* involves immediate membrane depolarization followed by slower rate of DNA destruction which differs from that observed for Gram-positive bacteria. Environ Microbiol 2012;14(7):1730–43. https://doi.org/10.1111/j.1462-2920.2011.02677.x. PMid: 22176893.
[10] Santo CE, Morais PV, Grass G. Isolation and characterization of bacteria resistant to metallic copper surfaces. Appl Environ Microbiol 2010;76(5):1341–8. https://doi.org/10.1128/AEM.01952-09.
[11] Salah I, Parkin IP, Allan E. Copper as an antimicrobial agent: Recent advances. RSC Adv 2021;11:18179–86. https://doi.org/10.1039/D1RA02149D. PMid: 35480904.
[12] Yaqoob AA, Ahmad H, Parveen T, et al. Recent advances in metal decorated nanomaterials and their various biological applications: A Review. Front Chem 2020;8:341. https://doi.org/10.3389/fchem.2020.00341. PMid: 32509720.
[13] Muñoz-Bonilla A, Fernández-García M. Polymeric materials with antimicrobial activity. Prog Polym Sci 2012;37(2):281–339. https://doi.org/10.1016/j.progpolymsci.2011.08.005.
[14] Ivanova EP, Hasan J, Webb HK, et al. Bactericidal activity of black silicon. Nat Commun 2013;4(1):2838. https://doi.org/10.1038/ncomms3838. PMid: 24281410.
[15] Ran B, Ran L, Wang Z, et al. Photocatalytic antimicrobials: Principles, design strategies, and applications. Chem Rev 2023;123(22):12371–430. https://doi.org/10.1021/acs.chemrev.3c00326. PMid: 37615679.
[16] Xie M, Gao M, Yun Y, et al. Antibacterial nanomaterials: Mechanisms, impacts on antimicrobial resistance and design principles. Angew Chem Int Ed 2023;62(17):e202217345. https://doi.org/10.1002/anie.202217345. PMid: 3671800.
[17] Linklater DP, Baulin VA, Juodkazis S, et al. Mechano-bactericidal actions of nanostructured surfaces. Nat Rev Microbiol 2021;19:8–22. https://doi.org/10.1038/s41579-020-0414-z. PMid: 32807981.
[18] Wang X, Shan M, Zhang S, et al. Stimuli-responsive antibacterial materials: Molecular structures, design principles, and biomedical applications. Adv Sci 2022;9(13):2104843. https://doi.org/10.1002/advs.202104843. PMid: 35224893.
[19] Duan S, Wu R, Xiong Y, et al. Multifunctional antimicrobial materials: From rational design to biomedical applications. Prog Mater Sci 2022;125:100887. https://doi.org/10.1016/j.pmatsci.2021.100887.
[20] Krzyżewska-Dudek E, Dulipati V, Kapczyńska K, et al. Lipopolysaccharide with long O-antigen is crucial for *Salmonella* Enteritidis to evade complement activity and to facilitate bacterial survival in vivo in the *Galleria mellonella* infection model. Med Microbiol Immunol 2024;213:8. https://doi.org/10.1007/s00430-024-00790-3.